



RESEARCH ARTICLE

DENSITY FUNCTIONAL THEORY STUDY OF STRUCTURAL, ELASTIC, ELECTRONIC AND OPTICAL PROPERTIES OF BiInO₃ CUBICPEROVSKITE MATERIAL

^{1,*}Paulos Tadesse Shibeshi and ²Tilahun Mulugeta

¹Department of Physics, College of Natural Science, Arba Minch University, Arba Minch, Ethiopia

²Kamba Secondary and Preparatory School, Kamba Woreda, Gamo Gofa Zone, Ethiopia

ARTICLE INFO

Article History:

Received 26th January, 2018

Received in revised form

08th February, 2018

Accepted 09th March, 2018

Published online 30th April, 2018

Key words:

Elastic property, Electronic Property, Optical property, Perovskite, Structure.

ABSTRACT

The structure, elastic, electronic and optical properties of cubic perovskite Bismuth Indium Oxide(BiInO₃) were calculated using full-potential linearized augmented plane wave method (FP-LAPW) in the density functional theory (DFT) using WIEN2k software. The calculated crystal structure of BiInO₃ revealed that this compound possesses cubic crystal structure with Fd-3m space group. The calculated band structure for BiInO₃ with generalized gradient approximations modified Becke-Johnson (GGA-mBJ) revealed the semiconducting behavior with an indirect band gap of 1.16 eV. It was also found that there exists a strong ionic bonding between Bi and O and a mixture of ionic and covalent bonding between In and O. The calculated elastic constants for BiInO₃ with generalized gradient approximations-Wu and Cohen (GGA-WC) method indicated that BiInO₃ is mechanically stable at ambient condition. To investigate the optical properties of BiInO₃ compound, the real and imaginary parts of the dielectric functions, refractive index, reflectivity spectra, extinction coefficient, optical absorption coefficient, electron energy loss function, and optical conductivity were also calculated with GGA-mBJ method in the photon energy range of 0 to 30 eV.

Copyright © 2018, Paulos Tadesse Shibeshi and Tilahun Mulugeta. This is an open access article distributed under the Creative Commons Attribution License, which permits unrestricted use, distribution, and reproduction in any medium, provided the original work is properly cited.

Citation: Paulos Tadesse Shibeshi and Tilahun Mulugeta, 2018. "Density functional theory study of structural, elastic, electronic and optical properties of BiInO₃ cubicperovskite Material", *International Journal of Current Research*, 10, (04), 68814-68819.

INTRODUCTION

Perovskites with general formula ABO₃ have been investigated intensively due to their wide range of interesting physical properties such as ferroelectricity, semi-conductivity, high temperature superconductivity, piezoelectricity, colossal magneto resistance and thermoelectricity (Ghosh *et al.*, 2015; Xiang *et al.*, 2005; Kumar *et al.*, 2008; Iles *et al.*, 2007). Moreover, they have been widely used as spintronic devices, optical waveguides, laser host crystals, high temperature oxygen sensors, frequency doubles, piezoelectric actuator materials and catalyst electrodes in certain types of fuel cells (Iles *et al.*, 2007; Verma and Jindal, 2009). BiInO₃ perovskite material has received considerable attention for producing ferroelectric and piezoelectric devices. It is a promising candidate for replacing Pb-based piezoelectric compounds due to similar piezoelectric properties. Few number of theoretical studies exploring structural, elastic and electronic properties of BiInO₃ compound have been carried out for the ideal cubic of the perovskite structure (Hai Wang *et al.*, 2007; Kaczowski and Jezierski, 2013). In this study, we have investigated the physical properties of BiInO₃ perovskite oxide by using

density functional theory. The structure, electronic, elastic and optical properties of this cubic perovskite material were calculated using FP-LAPW with local density approximation (LDA), GGA-mBJ and GGA-WC methods. It is expected that the present work will help in the understanding of physical behavior of BiInO₃ and the article will also cover the lack of theoretical data on the electronic, elastic and optical properties of this interesting compound.

Computational details

In this work, the calculations were conducted in the ideal cubic perovskite structure (space group #221) of BiInO₃ with atomic Wyckoff positions Bi (0,0,0), In (0.5, 0.5, 0.5) and O (0.5,0.5,0) as well as lattice constant $a_0 = 5.396 \text{ \AA}$. All the calculations were carried out using FP-LAPW method within the Wien2k computer code, based on the LDA, GGA-mBJ and GGA-WC approximations for the exchange-correlation potential within the framework of DFT (Blaha *et al.*, 2001). The muffin tin atomic sphere radii R_{MT} of Bi, In and O were set to be 2.0, 1.8 and 1.5 a.u., respectively. The Brillouin zone integration was performed by using the modified tetrahedron method up to 35 k-points in the irreducible part of the simple cubic Brillouin zone. The plane-wave expansion was controlled by setting $R_{MT} \times K_{MAX} = 7$ (where R_{MT} is the

*Corresponding author: Paulos Tadesse Shibeshi,

Department of Physics, College of Natural Science, Arba Minch University, Arba Minch, Ethiopia.

smallest of the muffin-tin radii and K_{MAX} is the plane wave cut-off the interstitial plane wave). The cut-off energy which defines the separation between the core and valence states was set at -9.0 Ry. For the total energy calculations, the energy convergence criterion was set to be 10^{-4} Ry. For k-space integration, 364 k-points in the entire Brillouin Zone were used.

RESULT AND DISCUSSION

Crystal structure calculation: The room temperature crystal structure of BiInO₃ is illustrated in Figure 1, where the cations Bi are shown at the corners of the cube, In cations in the center with oxygen ions in the face-centered positions. This indicates that, BiInO₃ attained cubic crystal structure. The calculated lattice energy as a function of volume per particle for BiInO₃ using GGA-WC method is shown in Figure 2. This calculation allowed the prediction of the most stable structure, equilibrium energy, unit cell volume, bulk modulus and its derivative of BiInO₃. The curve is obtained by fitting the Birch-Murnaghan equation given by (Souza and Rino, 2011);

$$E(V) = E_0 + \frac{9V_0 B_0}{16} \left\{ \left[\left(\frac{V_0}{V} \right)^{\frac{2}{3}} - 1 \right]^3 B_0' + \left[\left(\frac{V_0}{V} \right)^{\frac{2}{3}} - 1 \right]^2 \left[6 - 4 \left(\frac{V_0}{V} \right)^{\frac{2}{3}} \right] \right\}$$

where V_0 is the equilibrium volume, B_0 is the bulk modulus which is given by:

$$B_0 = -V \left(\frac{\delta P}{\delta V} \right)_T$$

and B_0' is the pressure derivative of B_0 evaluated at volume V_0 . This helps to determine the equilibrium

Table 1. The calculated structural parameters and ground state energy for BiInO₃ oxide

Method	a(Å)	V(Å ³)	B(GPa)	E ₀ (Ry)
LDA	4.0809	67.96	166.54	55341.24
GGA - WC	4.1204	69.95	156.18	55370.52
GGA - PBE	4.1691	72.46	136.54	- 55376.46

lattice constant of the compound by the minimization of the total energy of the system with respect to the volume of the unit cell. The Birch-Murnaghan equation, which is described above is also used to obtain the structural parameters: lattice parameter a , the unit cell volume V , the bulk modulus B and the ground state energy E_0 for BiInO₃ oxide. The obtained results are summarized in Table 1. For these purposes different approaches, i.e. LDA, GGA-PBE and GGA-WC were employed. Table 1. The calculated structural parameters and ground state energy for BiInO₃ oxide. It can be seen that the calculated values are not the same. The obtained results using LDA, GGA-WC and GGA-PBE methods are in good agreement with those calculated in (Verma and Jindal, 2009; Hai Wang et al., 2007; Kaczowski and Jezierski, 2013). However, as compared them, the lattice parameter calculated within LDA is slightly smaller than those from GGA-WC and GGA-PBE methods. As reported by A. D. Corso *et al.* (1996), GGA approximation overestimates the lattice constants and underestimates the bulk moduli. For all approximations, the bulk modulus values are inversely proportional to the calculated values of the lattice parameters, a , and the unit cell volume, V_0 . Similar results have been reported by J. Kaczowski and A. Jezierski (Kaczowski and Jezierski, 2013). Finally, we note that experimental result for the lattice

constant and bulk modulus of cubic BiInO₃ compound is not available.

Band structure and densities of states: The band structures along high symmetry directions in the Brillouin zone calculated with GGA-mBJ and densities of states (DOS) for BiInO₃ are shown in Figure 3 (I). The calculated band gaps are also summarized in Table 2. The valence band maximum (VBM) and the conduction band minimum (CBM) are occurred at M and X points, respectively. Moreover, the two bands are not overlapped each other, indicating that the material is an indirect semiconductor with band gap of 1.16 eV. To further explain the nature of the electronic band structure, the total (DOS) of BiInO₃ is calculated and the result is shown in Figure 3(II). On the basis of different bands, the total DOS could be grouped into four regions. The first region around -12.5 eV comprising a narrow band due to the $4d$ orbital states (Figure 3 (ii) b). In the second region around -10 eV to Fermi energy level, majority contribution is due to Bi $6s$ states (Figure 3 (ii) a). In the third region from -6 eV to Fermi level the major contribution is given by $6s$ and In $4f$ (Figure 3 (ii) c). There is hybridization between Bi $6s$ and In $4f$ with O $2p$ states in this region. The first, second and third regions within the range of -12.5 to 0.0 eV comprise the valence band. The upper part of the valence band is composed of the O $2p$ and Bi $6p$ states. The fourth region above the Fermi level is the conduction bands. In the conduction band from 2.54 to 8 eV majority contributions are from Bi $6p$ and O $2p$ states. From 10 to 20 eV, a small contribution is due to the O $2p$ and Bi $5f$ states in the conduction band.

Charge density: It is well known that the ionic character of any material can be related to the charge transfer between the cation and anion. On the other hand, the covalent character is related to the sharing of the charge among the cation and anion. In order to identify the bonding nature in BiInO₃ compound, we plot the calculated charge density -0.5 eV to E_F (0 eV) maps of (100) and (110) planes and the obtained results are shown in Figures 4. From Figure 4 (a), it is clearly observed that the near spherical charge distributions around Bi, which indicates the clear identifications of ionic bonding between Bi and O with no charge sharing. Further, it is obtained that there is a strong directional bonding between In and O in BiInO₃. This is due to the fact that most of the charges are populated in the In-O bond direction, while the maximum charge resides on the Bi and In sites. It is also obtained that the hybridization between In and O is stronger than hybridization between Bi and O, and are responsible for the covalent bonding (Figures 4 (b)). The covalent bonds are clearly visible in Figures 4, which is consistent with those obtained by Hai Wang *et al.* (2007). From the above observed results, we can conclude that there exists a strong ionic bonding between Bi and O, and a mixture of ionic and covalent bonding between In and O.

Elastic properties: The elastic constants of solids are important parameters which provide a link between the mechanical and dynamical behavior of crystals, and give important information concerning the response of the crystal to the external forces. In particular, they provide information on the mechanical strength of materials such as the structural stability and stiffness of materials. A hyperplastic material with stress and strain symmetry has 21 independent elastic constants, C_{ij} (Rameshe *et al.*, 2015). The material with 21 independent elastic constants is called as anisotropic or aelotropic material.

Table 2. The calculated band gap (eV) for BiInO₃ compound

Method	M-Γ	M-X	R-X	R-M	M-M	R-R	R-Γ	X-X
GGA-mBJ	4.4	1.16	1.16	2.45	2.45	4.3	4.4	2.2

Table 3. Calculated elastic parameters C_{ii}(GPa), anisotropy factor A, bulk modulus B (GPa), shear modulus G (GPa), Poisson's ratio ν, Young's modulus Y (GPa), Pugh'sindex B/G and Cauchy's pressure C₁₂- C₄₄ (GPa) of BiInO₂

Compound	C ₁₁	C ₁₂	C ₄₄	A	B	G	ν	Y	B/G	C ₁₂ - C ₄₄
BiInO ₃	292.4	89.4	48.4	0.48	157.07	65.42	0.32	172.33	2.4	41

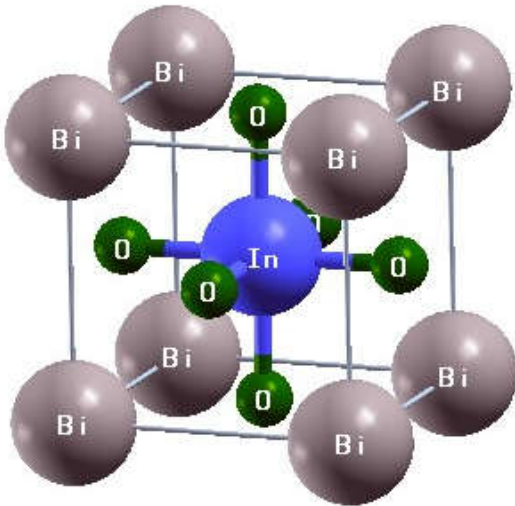


Figure 1. Crystal structure of a unit cell BiInO₃ perovskite

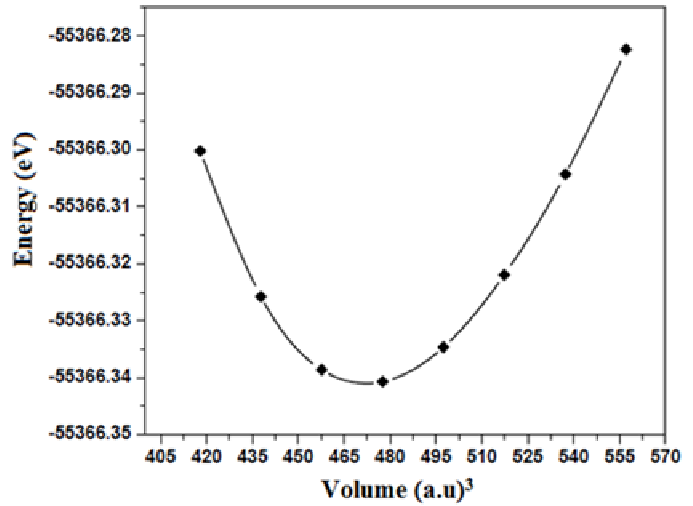


Figure 2. Total energy versus volume of BiInO₃

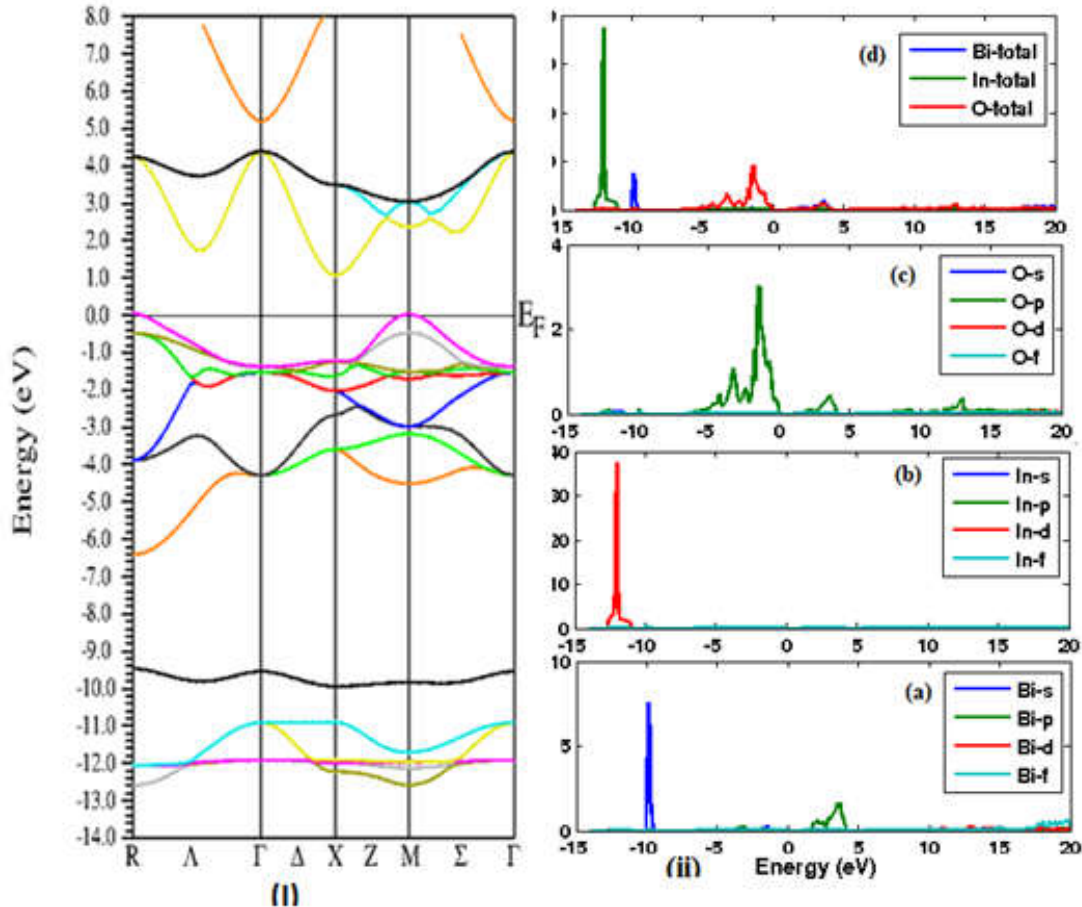


Figure 3. The calculated (i) band structure and (ii) density of states (DOS) of cubic BiInO₃

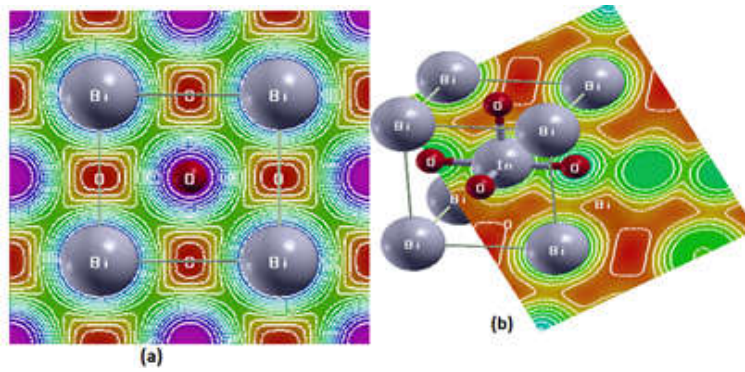


Figure 4. Charge density distribution of BiInO₃ (a) along (100) plane in 2-D representation, (b) along (110) plane in 2-D representation

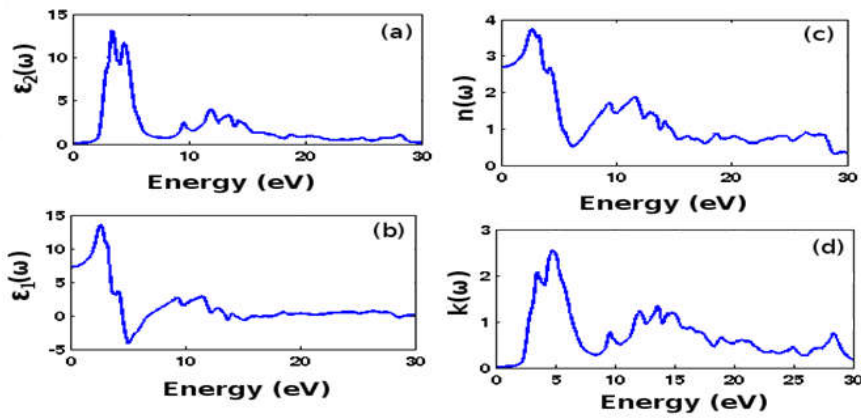


Figure 5. (a) imaginary part $\epsilon_2(\omega)$ (b) real part $\epsilon_1(\omega)$ (c) refractive index $n(\omega)$ (d) extinction coefficient $k(\omega)$ of BiInO₃

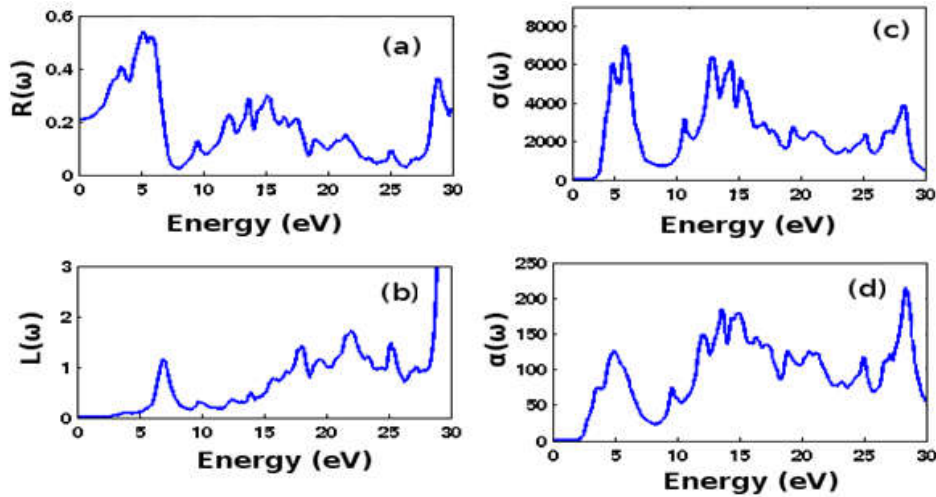


Figure 6. (a) reflectivity $R(\omega)$, (b) energy loss function $L(\omega)$, (c) optical conductivity $\sigma(\omega)$ and (d) absorption coefficient $\alpha(\omega)$ of BiInO₃

However, the symmetry of cubic crystals reduces this number to only three independent elastic moduli, C_{11} , C_{12} and C_{44} (Rameshe *et al.*, 2015) with the following identities $C_{11} = C_{22} = C_{33}$, $C_{12} = C_{23} = C_{31}$, and $C_{44} = C_{55} = C_{66}$ (Brik, 2010). In order to determine them, the cubic unit cell is deformed using an appropriate strain tensor to yield an energy-strain relation. In this work, we used the method developed by T. Charpin and implemented in the WIEN2K package (Blaha *et al.*, 2001). Once the single-crystal elastic constants C_{11} , C_{12} , and C_{44} are evaluated, related properties such as bulk modulus B , shear modulus G , Poisson's ratio ν , Young's modulus Y , Pugh's index B/G and Cauchy's pressure of polycrystalline can be estimated in terms of Voigt-Reuss-Hill approximations.

All these parameters were calculated using equations from (Faizan *et al.*, 2016). The obtained values for BiInO₃ using GGA-WC method are shown in Table 3. It is obtained that the calculated elastic constants C_{ij} are positive and satisfied the mechanical stability condition (Faizan *et al.*, 2016) in a cubic crystal, i.e. $(C_{11} - C_{12}) > 0$, $(C_{11} + 2C_{12}) > 0$, $C_{11} > 0$, $C_{44} > 0$, and $C_{12} < B < C_{11}$. This suggests that BiInO₃ compound is mechanically stable. Upon the calculation of the elastic constants, it is found that BiInO₃ exhibit the highest value of C_{11} , which is 83% higher than C_{44} . This reveals that BiInO₃ compound has weaker resistance to the pure shear deformation compared to the resistance to the unidirectional compression. This suggests that for cubic crystals elastic constants decrease

with increase of the lattice parameters. Similar result is obtained by M.G. Brik (Brik, 2010). The elastic anisotropy factor A in a cubic crystal is a measure of the degree of elastic anisotropy in solids. The elastic anisotropy factor takes the value of one for a completely isotropic material, while any value smaller or larger than one indicates elastic anisotropy possessed by the crystal (Brik, 2010). It can be observed in the Table 3 that the obtained value of the anisotropy factor is 0.48 for BiInO₃, which indicates that the compound is anisotropic material. Bulk modulus B is a measurement of the hardness of a solid, which is materials resistance to the volume change by an applied pressure. The calculated value of bulk modulus is 157.07 GPa for BiInO₃. This high value of the bulk modulus reflects a tendency for better ductility (brittleness) of BiGaO₃. The shear modulus G, describes the resistance of a material upon shape change. As it can be seen in the table, BiInO₃ has 65.42 GPa shear modulus value. The high shear modulus value is a better predictor of hardness of materials. Thus, from the obtained data it can be predicted that Perovskite BiInO₃ has large resistance to shape change to the external forces. Poisson's ratio provides more information about the bonding forces than any other elastic property. The value of the Poisson's ratio for covalent materials is small ($\nu < 0.1$), whereas for ionic materials a typical value of ν is 0.25 (Brik, 2010). In this calculation, the obtained value of the Poisson's ratio is 0.32. It can be assumed the presence of a considerable ionic contribution in intra-atomic bonding for BiInO₃ compound. Young's modulus is defined as the ratio of stress and strain, and used to provide a measure of the stiffness of the solid. The material is stiffer if the value of Young's modulus is high. It is clear from Table 3 that bulk modulus of BiInO₃ is 65.42 GPa. Mechanical properties such as ductility and brittleness of materials can be explained from the proposed relationship in Pugh's criteria. The shear modulus G represents the resistance to plastic deformation, while the bulk modulus B represents the resistance to fracture. We know that there is a criterion for B/G ratio which separates the ductility and brittleness of materials. According to Ephraim Babu *et al.* (2014), the critical value for B/G ratio is 1.75, i.e. if $B/G > 1.75$ the material is ductile, otherwise it is brittle. As it can be seen in Table 3, the obtained result is 2.4. Hence, we can deduce that BiInO₃ compound possesses ductile nature. It has been also noted that the Cauchy pressure $C_{12} - C_{44} < 0$ for covalent compounds and $C_{12} - C_{44} > 0$ for mostly ionic compounds (Brik, 2010). As shown in the table 3, the obtained values of Cauchy pressure 41 (GPa), leading to BiInO₃ compound is mostly ionic crystals.

Optical properties: The optical properties of the perovskites can be described by the electronic dielectric function $\epsilon(\omega)$. The dielectric function $\epsilon(\omega)$ describes the optical response of the medium to the incident photons with an energy $E = \hbar\omega$. In terms of the complex dielectric function $\epsilon(\omega)$, the dielectric function of an anisotropic material can be expressed as;

$$\epsilon(\omega) = \epsilon_1(\omega) + i\epsilon_2(\omega)$$

where $\epsilon_1(\omega)$ and $i\epsilon_2(\omega)$ are the real and imaginary components of the dielectric function, respectively. The imaginary part of the frequency dependent dielectric function is given by (Ephraim Babu *et al.*, 2014);

$$\epsilon_2(\omega) = \left(\frac{e^2 \hbar}{\pi m^2 \omega^2} \right) \sum_{ij} \int d^3k [M_{ij}(k)]^2 \delta(E_{ik} - E_{jk} - \omega)$$

where M_{ij} is the dipole matrix, i and j are the initial and final states respectively, the energy $\hbar\omega_{ij} = E_{ik} - E_{jk}$ is the energy of electron in the ij -th states with crystal wave vector k . Further, the real part of the dielectric function ϵ_1 can be derived from the imaginary part ϵ_2 using the Kramers-Kronig relations (Ephraim Babu *et al.*, 2014).

$$\epsilon_1(\omega) = 1 + \frac{2}{\pi} P \int_0^{\infty} \frac{\omega' \epsilon_2(\omega') d\omega'}{\omega'^2 - \omega^2}$$

where, P implies the principal value of the integral. From $\epsilon_1(\omega)$ and $\epsilon_2(\omega)$, the rest frequency dependent optical functions, such as refractive index $n(\omega)$, reflectivity spectra $R(\omega)$, extinction coefficient $k(\omega)$, optical absorption coefficient $I(\omega)$ and electron energy loss function $L(\omega)$ and optical conductivity $\sigma(\omega)$ were calculated using equations from (Kong *et al.*, 2017; Ephraim Babu *et al.*, 2012). The optical properties of BiInO₃ was also calculated at equilibrium lattice parameters using mBJ-GGA method in the photon energy range 0 to 30 eV. The obtained results are shown in Figures 5 and 6 (a-d). As shown in Figure 5 (a), a strong absorption peak is obtained in the energy range of 2.3 - 20.0 eV. The maximum absorption peak of the dielectric function is occurred at 3.4 eV, which is related to the transition of the interband between the valence band maximum and the conduction band minimum. The maximum peak of the dielectric function is occurred at 2.5 eV, due to the transition of 2p electrons of O in the highest valence band maximum into 6p electrons in the lowest conduction band of Bi. The peaks beyond 2.5 eV are appeared due to the electronic transition from the O 2p states in valence band to the Bi 6p states in the unoccupied conduction bands.

The variation of the real part of the dielectric function $\epsilon_1(\omega)$ with the incident photon energy up to 30 eV is shown in Figure 5 (b). It is observed that the static dielectric constant at zero frequency limit $\epsilon_1(0)$ of BiInO₃ is found to be 2.5, which is lower than that of BiGaO₃. Beyond the zero frequency limit, $\epsilon_1(\omega)$ increases and reaches a maximum value of 4.9 at 7.4 eV. Further the plot decreases sharply and goes below 0.0 eV in the range of 15.2 - 20.5 eV and 27.2 - 28.3 eV. For negative values of $\epsilon_1(\omega)$, BiInO₃ is characterized as metals and it lost the dielectric property. The calculated values of $n(\omega)$ and $k(\omega)$ of BiInO₃ are shown in Figure 5 (c) and (d). From the figure it clear that $n(\omega)$ and $k(\omega)$ have almost the same characteristics as $\epsilon_1(\omega)$ and $\epsilon_2(\omega)$, respectively. The peaks in $\epsilon_2(\omega)$ and $k(\omega)$ are due to the inter-band electronic transitions. The static dielectric constant at zero frequency limit $n(0)$ of BiInO₃ is found to be 2.6. Beyond the zero-frequency limit, $n(\omega)$ start increasing and reaches a maximum value of 3.8 at 2.8 eV. After its maximum value, $n(\omega)$ starts decreasing and becomes almost constant after 15 eV. Further, the calculated $k(\omega)$ shows the same behavior as $\epsilon_2(\omega)$. As shown in Figure 5 (d), the frequency dependent $k(\omega)$ increases monotonically and reaches the maximum absorption in the medium at 4.9 eV, indicating the fast absorption of photons by BiInO₃. Further, it is also found that $\epsilon_1(\omega)$ shows lower value at the maximum value of $k(\omega)$. Figure 6 (a) shows the optical reflectivity $R(\omega)$ versus energy for BiInO₃. It is found that the zero-frequency reflectivity $R(0)$ is found to be 21 %. The maximum reflectivity value is about 54.2 % occurs at 5.2 eV. In this case the maximum reflectivity occurs when its corresponding $\epsilon_1(\omega)$ is below zero. The energy loss Figure 6 (a-d): (a) reflectivity

$R(\omega)$, (b) energy loss function $L(\omega)$, (c) optical conductivity $\sigma(\omega)$ and (d) absorption coefficient $\alpha(\omega)$ of BiInO₃. spectra $L(\omega)$ for BiInO₃ is shown in Figure 6 (b). It is obtained that the maximum peak is located at 22 eV. The optical conductivity $\sigma(\omega)$ of BiInO₃ is shown in Figure 6 (c). The maximum value of optical conductivity of the compound is obtained at 6 eV of magnitude $6947.3 \Omega^{-1}\text{cm}^{-1}$. Similar results are also observed in absorption coefficient $\alpha(\omega)$ in the absorption range up to 30 eV and it is shown in Figure 6 (d). The maximum absorption occurs at 28 eV, making the materials more favorable for applications in optoelectronic devices.

Conclusion

The application of DFT as implemented in WIEN2K code is successfully predicting the structural, elastic, electronic, and optical properties of the cubic BiInO₃ perovskite using the FP-LAPW method within the LDA, GGA in the framework of DFT. From band structure calculation, it is found that BiInO₃ perovskites exhibit semiconducting behavior with an indirect band gap structure. From elastic properties study, it is obtained that the calculated elastic constants C_{ij} are positive. This suggests that BiInO₃ is mechanically stable compound. From optical properties study, it is also suggested that BiInO₃ is more favorable for applications in optoelectronic devices.

Conflict of interests: This research has not been submitted for publication nor has it been published in whole or in part elsewhere. We attest to the fact that both authors listed on the title page have contributed significantly to the work, have read the manuscript, attest to the validity and legitimacy of the data and its interpretation, and agree to its submission to the OMO International Journal of Sciences.

REFERENCES

Blaha, P., Schwarz, K., Madsen, G.K.H., Kvasnicka, D. and Luitz, J. 2001. An WIEN2K, Augmented-Plane-Wave + Local Orbitals Program for Calculating Crystal properties, Karlheinz Schwarz, Techn.,Wien.

Brik, M.G. 2010. First-principles calculations of electronic, optical and elastic properties of ZnAl₂S₄ and ZnGa₂O₄. *Journal of Physics and Chemistry*, 71(10), 1435.

Corso, A. D., Pasquarello, A., Baldereschi, A. and Car, R. 1996. Generalized-gradient approximations to density-functional theory: A comparative study for atoms and solids. *Journal of Physical Review*, B, 53: 1180.

Ephraim Babu, K., Murali, N., Vijaya Babu, K., Paulos Tadesse, V. and Veeraiah, 2014. Structural, elastic,

electronic, and optical properties of cubic perovskite CsCaCl₃ compound: an ab initio study. *Acta Physica Polonica*, 125 (5): (2014).

Ephraim Babu, K., Veeraiah, A., Tirupati Swamy, D. and Veeraiah, V. 2012. First-Principles Study of Electronic Structure and Optical Properties of Cubic Perovskite CsCaF₃. *Chinese Physics Letter*, 29(11): 1-5.

Faizan, M., Murtaza, G., Azam, S., Ayaz Khan, S., Mahmood, A. and Yar, A. 2016. Elastic and optoelectronic properties of novel Ag₃AuSe₂ and Ag₃AuTe₂ semiconductors. *Materials Science in Semiconductor Processing*, 52: 8–15.

Ghosh, S., Sante, D. D. and Stroppa, A. 2015. Strain tuning of ferroelectric polarization in hybrid organic inorganic perovskite compounds. *The journal of physical chemistry letters*, 6(22): 4553-4559.

Hai Wang, Biao Wang, Qingkun Li, Zhenye Zhu, Rui Wang and Woo, C. H. 2007. First-principles study of the cubic perovskites BiMO₃ (M=Al, Ga, In, and Sc). *Physical Review B*, 75: 1-10.

Iles, N., Kellou, A., Driss Khodja, K., Amrani, B., Lemoigno, F., Bourbie, D. and Aourag, H. 2007. Atomistic study of structural, elastic, electronic and thermal properties of perovskites Ba(Ti,Zr,Nb)O₃. *Computational Materials Science*, 39: 896–902.

Kaczkowski, J. and Jezierski, A. 2013. Electronic Structure of the Cubic Perovskites BiMO₃ (M = Al, Ga, In, Sc). *Acta Physica Polonica A*, 124(3): 852-854.

Kong, X., Yuan, Z., Yu, Y., Gao, T. and Ma, S. 2017. Elastic, vibrational, and thermodynamic properties of Sr₁₀(PO₄)₆F₂ and Ca₁₀(PO₄)₆F₂ from first principles. *Chin. Phys. B*, 26(8): 1-9.

Kumar, A., Verma, A. S. and Bhardwaj, S.R. 2008. Prediction of formability in perovskite-type oxides. *Applied Physics Journal*, 1: 11-19.

Ramesh, B., Rajagopalan, M. and Palanivel, B. 2015. Electronic structure, structural phase stability, optical and thermoelectric properties of Sr₂AlM'O₆ (M' = Nb and Ta) from first principle calculations. *Computational Condensed Matter*, 4: 13-22.

Souza, J.A. and Rino, J.P. 2011. Molecular dynamics study of structural and dynamical correlations of CaTiO₃. *Acta Materialia*, 59: 1409–1423.

Verma, A.S. and Jindal, V.K. 2009. Lattice constant of cubic perovskites. *Journal of Alloys and Compounds*, 485: 514–518.

Xiang, W., Yuhui, D., Shan, Q., Mamatimin, A. and Ziyu W. 2005. First-principles study of the pressure-induced phase transition in CaTiO₃. *Solid State Communications*, 136: 416–420.
